Material parameter retrieval procedure for general bi-isotropic metamaterials and its application to optical chiral negative-index metamaterial design

Do-Hoon Kwon,[1] **Douglas H. Werner,**[1,*] **Alexander V. Kildishev,**[2] **and Vladimir M. Shalaev**[2]

[1]*Department of Electrical Engineering, Pennsylvania State University University Park, Pennsylvania 16802, USA*

[2]*Birck Nanotechnology Center, School of Electrical and Computer Engineering Purdue University, West Lafayette, Indiana 47907, USA*

dhw@psu.edu

Abstract: A chiral optical negative-index metamaterial design of doubly periodic construction for the near-infrared spectrum is presented. The chirality is realized by incorporating sub-wavelength planar silver-alumina-silver resonators and arranging them in a left-handed helical (i.e., stair-step) configuration as a wave propagates through the metamaterial. An effective material parameter retrieval procedure is developed for general bi-isotropic metamaterials. A numerical design example is presented and the retrieved effective material parameters exhibiting a negative index of refraction are provided.

OCIS codes: (160.4760) Optical properties; (260.5430) Polarization; (310.6860) Thin films, optical properties

References and links

1. I. V. Lindell, A. H. Sihvola, S. A. Tretyakov, and A. J. Viitanen, *Electromagnetic Waves in Chiral and Bi-Isotropic Media* (Artech House, Boston, 1994).
2. J. B. Pendry, "Negative refraction makes a perfect lens," Phys. Rev. Lett. **85**, 3966–3969 (2000).
3. R. A. Shelby, D. R. Smith, and S. Schultz, "Experimental verification of a negative index of refraction," Science **292**, 77–79 (2001).
4. S. Zhang, W. Fan, K. J. Malloy, S. R. J. Brueck, N. C. Panoiu, and R. M. Osgood, "Near-infrared double negative metamaterials," Opt. Express **13**, 4922–4930 (2005).
5. G. Dolling, M. Wegener, C. M. Soukoulis, and S. Linden, "Negative-index metamaterial at 780 mm wavelength," Opt. Lett. **32**, 53–55 (2007).
6. U. K. Chettiar, A. V. Kildishev, H.-K. Yuan, W. Cai, S. Xiao, V. P. Drachev, and V. M. Shalaev, "Dual-band negative index metamaterial: double negative at 813nm and single negative at 772nm," Opt. Lett. **32**, 1671–1673 (2007).
7. J. B. Pendry, "A chiral route to negative refraction," Science **306**, 1353–1355 (2004).
8. V. Yannopapas, "Negative index of refraction in artificial chiral materials," J. Phys.: Condens. Matter **18**, 6883–6890 (2006).
9. Y. Svirko, N. Zheludev, and M. Osipov, "Layered chiral metallic microstructures with inductive coupling," Appl. Phys. Lett. **78**, 498–500 (2001).
10. A. V. Rogacheva, V. A. Fedotov, A. S. Schwanecke, and N. I. Zheludev, "Giant gyrotropy due to electromagnetic-field coupling in a bilayered chiral structure," Phys. Rev. Lett. **97**, 177401 (2006).
11. E. Plum, J. Dong, J. Zhou, V. A. Fedotov, T. Koschny, C. M. Soukoulis, and N. I. Zheludev, "3D-chiral metamaterial showing artificial magnetic response and negative refraction," arXiv:0806.0823v1 (2008).

#95702 - $15.00 USD Received 2 May 2008; revised 29 Jun 2008; accepted 1 Jul 2008; published 23 Jul 2008

12. E. Plum, V. A. Fedotov, A. S. Schwanecke, N. I. Zheludev, and Y. Chen, "Giant optical gyrotropy due to electromagnetic coupling," Appl. Phys. Lett. **90**, 223113 (2007).
13. M. Decker, M. W. Klein, M. Wegener, and S. Linden, "Circular dichroism of planar chiral magnetic metamaterials," Opt. Lett. **32**, 856–858 (2007).
14. D. R. Smith, S. Schultz, P. Markoš, and C. M. Soukoulis, "Determination of effective permittivity and permeability of metamaterials from reflection and transmission coefficients," Phys. Rev. B **65**, 195104 (2002).
15. A. V. Kildishev and U. K. Chettiar, "Cascading optical negative index metamaterials," Appl. Comput. Electrom. **22**, 172–183 (2007).
16. M. Kuwata-Gonokami, N. Saito, Y. Ino, M. Kauranen, K. Jefimovs, T. Vallius, J. Turunen, and Y. Svirko, "Giant optical activity in quasi-two-dimensional planar nanostructures," Phys. Rev. Lett. **95**, 227401 (2005).
17. D.-H. Kwon, P. L. Werner, and D. H. Werner, "Optical planar chiral metamaterial designs for strong circular dichroism and polarization rotation," Opt. Express **16**, 11802–11807 (2008).
18. J. L. Volakis, A. Chatterjee, and L. C. Kempel, *Finite Element Method for Electromagnetics* (IEEE Press, Piscataway, NJ, 1998).
19. P. B. Johnson and R. W. Christy, "Optical constants of the noble metals," Phys. Rev. B **6**, 4370–4379 (1972).
20. E. D. Palik, ed., *Handbook of Optical Constants of Solids II* (Academic Press, Boston, 1991).
21. B. Bai, Y. Svirko, J. Turunen, and T. Vallius, "Optical activity in planar chiral metamaterials: Theoretical study," Phys. Rev. A **76**, 023811 (2007).

1. Introduction

A chiral structure refers to a geometrical configuration that cannot be brought into congruence with its own mirror image. Isotropic chiral media are a subset of the general bi-isotropic (BI) media, for which the constitutive relations among electromagnetic vector quantities **E**, **H**, **D**, and **B** are described by [1]

$$\mathbf{D} = \varepsilon\mathbf{E} + (\chi + i\kappa)\sqrt{\mu_0\varepsilon_0}\mathbf{H}, \tag{1}$$

$$\mathbf{B} = (\chi - i\kappa)\sqrt{\mu_0\varepsilon_0}\mathbf{E} + \mu\mathbf{H}, \tag{2}$$

where χ and κ are the Tellegen and the chirality parameters, respectively. Unlike in isotropic media, the polarization ellipse of a plane wave rotates as it propagates with a modified phase velocity in BI media with non-zero values for χ and κ. The Tellegen parameter χ affects the phase propagation of the plane wave, but not the polarization rotation. The reverse is true for the chirality parameter κ [1].

Since novel applications including a perfect lens [2] were predicted and the phenomenon of negative refraction was experimentally demonstrated [3], negative-index metamaterials (NIMs) have garnered considerable interest in the science and engineering communities. A typical NIM design in the optical regime consists of a metal-dielectric-metal sandwich structure with perforations [4, 5, 6]. Negative effective permittivity values are provided by the continuous metal mesh structure. The two metal strips separated by a dielectric layer provide negative permeability values by utilizing magnetic resonances. The vast majority of optical metamaterial designs reported to date are not chiral structures.

Recently, a metamaterial design philosophy for realizing negative refractive indices using sub-wavelength chiral inclusions [7] has been proposed. A theoretical chiral NIM design at optical wavelengths was presented in [8]. The index of refraction $n_\pm$ for the right-hand circularly polarized (RCP,+) and the left-hand circularly polarized (LCP,−) components in a homogeneous, isotropic chiral medium may be expressed as $n_\pm = n \pm \kappa$, where $n = \sqrt{\mu\varepsilon/\mu_0\varepsilon_0}$ [1]. These proposed design approaches aim at realizing a strong artificial chirality such that one of the two circularly polarized components has a negative index of refraction. This NIM design approach using strong chirality does not require the strong resonance conditions which are typically utilized in non-chiral NIM designs. Since a strong resonance entails undesirable absorption of energy as a wave propagates through the NIM, the design approach utilizing chirality promises to be an effective methodology that can potentially lead to NIM realizations with significantly reduced absorption loss compared with conventional non-chiral NIM designs.

#95702 - $15.00 USD Received 2 May 2008; revised 29 Jun 2008; accepted 1 Jul 2008; published 23 Jul 2008

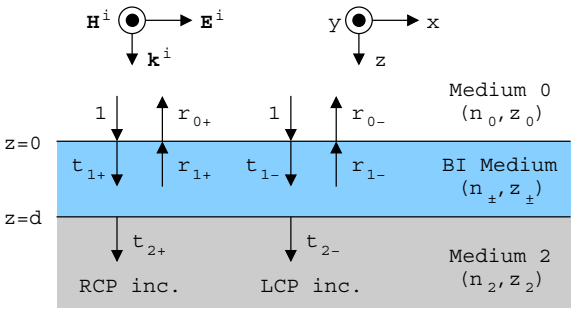

Fig. 1. (Color online) A BI slab under illumination by a circularly-polarized plane wave.

In 2001, strong optical activity and circular dichroism were predicted and analyzed in terms of effective medium theory for quasi-planar chiral metallic structures with inductive coupling [9]. The "signature" of negative refraction, i.e. the phase and group velocities extracted from the transmitted field having opposite signs, was experimentally observed for one circular polarization from a bilayered chiral structure in the microwave band [10]. Experimental verification of chiral negative refraction was extended to a three-dimensional multilayer chiral metamaterial design [11]. A similar bilayered chiral structure in the optical regime was reported to exhibit strong optical activity in [12]. For a double-layer planar chiral metamaterial design that supports strong magnetic-dipole moments, enhanced circular dichroism was experimentally observed at near-infrared wavelengths [13].

This paper presents a chiral NIM slab design in the near-infrared (near-IR) spectrum. First, the effective material parameter retrieval procedure for a general BI metamaterial is presented, which is based on an extension of the inversion approach for non-chiral metamaterials reported in [14, 15]. Following this, an optical NIM design incorporating magnetic resonators of chiral construction is introduced and the full-wave analysis results for this structure are presented.

2. BI material parameter inversion

For a given BI metamaterial slab, we can define the equivalent index of refraction $n_\pm$ and the impedance $z_\pm$ for the RCP and the LCP components. Their values correspond to those of a homogeneous BI slab that produces the identical transmission and reflection coefficients as the original slab.

Consider a homogeneous BI slab of thickness d which is illuminated by a normally incident plane wave. This is depicted in Fig. 1, where an RCP/LCP $(+/-)$ incident field impinges on the BI slab from the homogeneous isotropic medium 0 above it having material parameters (n_0, z_0). The BI slab is placed on the homogeneous isotropic half-space (medium 2) with material parameters (n_2, z_2). Based on the values of the reflection and transmission coefficients $r_{0\pm}$ and $t_{2\pm}$ assessed at the top and the bottom interfaces for the two circular polarizations, it is desired that the effective material parameters $(n_\pm, z_\pm)$ of the BI slab be recovered. The transmission and reflection coefficients inside the BI medium referenced at the $z = 0$ plane are denoted by $t_{1\pm}$ and $r_{1\pm}$, respectively.

Enforcing the continuity of tangential electric fields at the top interface for the two circular polarizations, one obtains

$$1 + r_{0\pm} = t_{1\pm} + r_{1\pm}, \tag{3}$$

$$\frac{1 - r_{0\pm}}{z_0} = \frac{t_{1\pm}}{z_\pm} - \frac{r_{1\pm}}{z_\mp}. \tag{4}$$

#95702 - $15.00 USD Received 2 May 2008; revised 29 Jun 2008; accepted 1 Jul 2008; published 23 Jul 2008

Note that the reflected wave propagates in the $-\hat{z}$ direction inside the BI medium and sees an impedance associated with the other handedness different from that of the incident wave. This is represented by the impedance $z_{\mp}$ in the denominator of the reflection term in (4). Next, enforcing the continuity of tangential electric and magnetic fields at the bottom interface yields

$$t_{1\pm}e^{ik_{\pm}d} + r_{1\pm}e^{-ik_{\mp}d} = t_{2\pm}, \tag{5}$$

$$\frac{t_{1\pm}e^{ik_{\pm}d}}{z_{\pm}} - \frac{r_{1\pm}e^{-ik_{\mp}d}}{z_{\mp}} = \frac{t_{2\pm}}{z_2}. \tag{6}$$

From (3)–(6), the quantities $t_{1\pm}$ and $r_{1\pm}$ can be eliminated. After some algebraic manipulations, one finds

$$e^{\mp ik_{\pm}d} = \frac{(1-r_{0+})/z_0 \pm (1+r_{0+})/z_{\mp}}{t_{2+}(1/z_2 \pm 1/z_{\mp})}, \tag{7}$$

$$e^{\mp ik_{\mp}d} = \frac{(1-r_{0-})/z_0 \pm (1+r_{0-})/z_{\pm}}{t_{2-}(1/z_2 \pm 1/z_{\pm})}, \tag{8}$$

where $k_{\pm}$ denotes the wavenumber for the RCP/LCP component within the homogenized BI medium. From (7)–(8), one finally obtains a quadratic equation for $1/z_{\pm}$ and a transcendental equation for $k_{\pm}$, which are given by

$$[(1+r_{0+})(1+r_{0-}) - t_{2+}t_{2-}]\left(\frac{1}{z_{\pm}}\right)^2 + \frac{2(r_{0\pm}-r_{0\mp})}{z_0}\left(\frac{1}{z_{\pm}}\right) - \frac{(1-r_{0+})(1-r_{0-})}{z_0^2} + \frac{t_{2+}t_{2-}}{z_2^2} = 0, \tag{9}$$

$$\cos k_{\pm}d = \frac{1}{2}\left[\frac{(1-r_{0\pm})/z_0 + (1+r_{0\pm})/z_{\mp}}{t_{2\pm}(1/z_2 + 1/z_{\mp})} + \frac{(1-r_{0\mp})/z_0 - (1+r_{0\mp})/z_{\mp}}{t_{2\mp}(1/z_2 - 1/z_{\mp})}\right]. \tag{10}$$

Eqs. (9)–(10) can be solved for $z_{\pm}$ and $n_{\pm}$, which can then be converted into the equivalent parameters z, n, χ, and κ using the relations

$$z = \sqrt{z_+ z_-}, \;\; n = (n_+ + n_-)\frac{z}{z_+ + z_-}, \;\; \chi = n\frac{z_+ - z_-}{i2z}, \;\; \kappa = \frac{n_+ - n_-}{2}. \tag{11}$$

During the solution process of (10), proper care should be exercised to select the correct branch for the real part of the arccosine function, similar to approaches that have been employed for non-chiral inversion procedures.

The material parameter inversion equations (9)–(10) are generalizations of the non-chiral retrieval procedures in [14, 15]. If isotropic material parameters are chosen in (1)–(2) such that $\chi = \kappa = 0$, it follows that $r_{0+} = r_{0-}$, $t_{2+} = t_{2-}$, and also $z_+ = z_-$, $n_+ = n_-$. Under these conditions, Eqs. (9)–(10) revert back to the familiar inversion equations for isotropic metamaterials [14, 15].

3. Chiral metamaterial design

Figure 2 illustrates the construction of a doubly-periodic chiral NIM in the near-IR regime. One quadrant of the unit cell is illustrated in Fig. 2(a). It is a union of four magnetic resonators, each of which is composed of an alumina (Al_2O_3) layer of thickness t_s sandwiched between two silver (Ag) layers of thicknesses t_t and t_b. The thickness of the alumina spacer is fixed at t_s but its vertical location is shifted in the $+\hat{z}$ direction at every 90° rotation in the counter-clockwise sense. This procedure is illustrated in Fig. 2(b), where only the alumina spacer layer

#95702 - $15.00 USD Received 2 May 2008; revised 29 Jun 2008; accepted 1 Jul 2008; published 23 Jul 2008

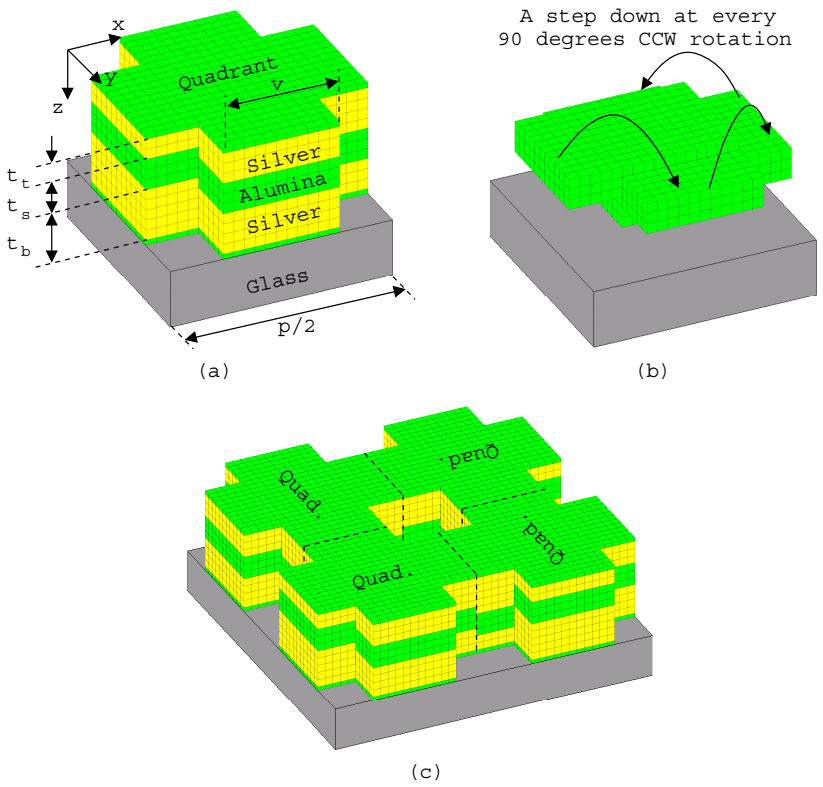

Fig. 2. (Color online) Construction of the unit cell of a doubly-periodic optical chiral metamaterial: (a) A quadrant, (b) The spacer layer geometry of a quadrant, (c) The unit cell.

of a quadrant is shown. The values of t_t and t_b are adjusted such that the total resonator thickness $t_t + t_s + t_b$ remains constant and the structure is unchanged when viewed from either of the $\pm\hat{z}$ directions. We note that the latter is characteristic of bulk-type chiral materials and this property is not shared by recently-discussed planar chiral metamaterials [16, 17]. A protective alumina layer of 10 nm thickness is applied on both sides.

The first quadrant is rotated by 90° and interconnected in sequence until the unit cell for the metamaterial shown in Fig. 2(c) is formed. This built-in rotational symmetry guarantees that the reflected and transmitted waves retain circular polarization states, which is characteristic of wave propagation in BI media. If the circular polarization states are not preserved upon reflection and transmission from the metamaterial, it cannot be equivalently represented by a homogeneous BI slab. Finally, the metamaterial is placed on a thick glass substrate, which is treated as a half space in the simulation.

The metamaterial is illuminated by circularly-polarized plane waves propagating in the $+\hat{z}$ direction. This electromagnetic scattering problem is rigorously solved using the finite element-boundary integral technique [18] with periodic boundary conditions. Alumina and glass are treated as lossless dielectric materials with constant relative permittivity values of 2.6244 and 2.25, respectively. The measured permittivity values reported in [19] are used to represent the silver. Material loss is detrimental to the overall performance of the NIM, especially at the locations where high field values are expected around the resonance wavelength. At visible and near-IR wavelengths, the metal losses in silver are much higher than the dielectric losses in alumina. Therefore, the lossless assumption for alumina at the design wavelength range is

#95702 - $15.00 USD Received 2 May 2008; revised 29 Jun 2008; accepted 1 Jul 2008; published 23 Jul 2008

justified. Moreover, alumina is also practically lossless at near-IR wavelengths [20].

It is noted that this chiral NIM design utilizes the characteristic features of bulk chiral materials and conventional non-chiral optical NIMs. Namely, both the helical feature of the structure and the planar resonators are incorporated into the design. The negative index response therefore will rely on a combination of the two features.

4. Numerical results

Prior to applying the BI material parameter inversion procedure developed in Section 2 to the chiral metamaterial design, we first establish that the two circular polarizations are indeed the eigenstates of the BI slab. In other words, we verify that the RCP and the LCP states are preserved upon transmission. For an $\hat{x}$- and a $\hat{y}$-directed linearly-polarized incident field, each of strength 1, let the transmitted fields be denoted by $\mathbf{E}_{tx}$ and $\mathbf{E}_{ty}$, respectively, such that

$$\mathbf{E}_{tx} = \hat{x}t_{xx} + \hat{y}t_{yx}, \tag{12}$$

$$\mathbf{E}_{ty} = \hat{x}t_{xy} + \hat{y}t_{yy}. \tag{13}$$

By introducing the unit vectors $\hat{u}_R = (\hat{x}+i\hat{y})/\sqrt{2}$ and $\hat{u}_L = (\hat{x}-i\hat{y})/\sqrt{2}$ for the RCP and the LCP waves propagating in the $+\hat{z}$ direction, the transmitted fields associated with the two incident wave polarizations having electric fields of unit strength can be written as

$$\mathbf{E}_{tR} = (\hat{x}\cdot\hat{u}_R)\mathbf{E}_{tx} + (\hat{y}\cdot\hat{u}_R)\mathbf{E}_{ty} = \hat{x}\frac{t_{xx}+it_{xy}}{\sqrt{2}} + \hat{y}\frac{t_{yx}+it_{yy}}{\sqrt{2}} = \hat{x}\frac{t_{xx}-it_{yx}}{\sqrt{2}} + \hat{y}\frac{t_{yx}+it_{xx}}{\sqrt{2}}, \tag{14}$$

$$\mathbf{E}_{tL} = (\hat{x}\cdot\hat{u}_L)\mathbf{E}_{tx} + (\hat{y}\cdot\hat{u}_L)\mathbf{E}_{ty} = \hat{x}\frac{t_{xx}-it_{xy}}{\sqrt{2}} + \hat{y}\frac{t_{yx}-it_{yy}}{\sqrt{2}} = \hat{x}\frac{t_{xx}+it_{yx}}{\sqrt{2}} + \hat{y}\frac{t_{yx}-it_{xx}}{\sqrt{2}}. \tag{15}$$

In (14)–(15), the relationships $t_{yy} = t_{xx}$ and $t_{xy} = -t_{yx}$ have been used, which follow from the four-fold rotational symmetry of the metamaterial structure for normal incidence. From (14)–(15), it can be easily seen that $\hat{u}_L^* \cdot \mathbf{E}_{tR} = 0$ and $\hat{u}_R^* \cdot \mathbf{E}_{tL} = 0$, whereas $\hat{u}_R^* \cdot \mathbf{E}_{tR} \neq 0$ and $\hat{u}_L^* \cdot \mathbf{E}_{tL} \neq 0$, which signifies that the transmitted waves $\mathbf{E}_{tR}$ and $\mathbf{E}_{tL}$ have purely RCP and LCP states. These two orthogonal relations have also been confirmed by numerical simulations (results not shown). Therefore, the effective medium description of the metamaterial is justified for normally incident plane wave illumination.

The effective material parameters for an example design are shown in Fig. 3. The values of the geometrical parameters used in this design are chosen to be $p = 840$ nm, $v = 220$ nm, $t_s = 60$ nm, and $t_t + t_b = 140$ nm, which results in a total thickness d of the metamaterial equal to 220 nm.

The reflection coefficients $r_{0\pm}$ are found to be the same, which leads to the same reflectances $R_\pm$ in Fig. 3(a) and identical impedances $z_\pm$ via (9) for the two circular polarizations as seen in Fig. 3(b). This agrees well with the conclusion based on the reciprocity principle for rotationally symmetric metamaterials under normal incidence conditions [21]. The difference in the transmission coefficients $t_{2\pm}$ leads to the different results for $n_\pm$ shown in Fig. 3(c). It is observed that a NIM band exists in the 0.978–1.11 μm wavelength range for the RCP component only. In sharp contrast, n_- steeply increases for the LCP component while n_+ decreases toward negative values as the wavelength is decreased. At the wavelength of the strongest negative index behavior, $\lambda = 1.015$ μm, the effective BI material parameters are found to be $n_+ = -1.78 + i1.80$, $z_+ = 0.023 - i0.43$, $\kappa = -2.10 - i0.07$, and $\chi = 0$. It can be observed that the wavelength of strongest chirality (i.e., maximum $|\kappa|$) is found to be $\lambda = 0.975$ μm, which is different from that of the strongest negative index band. The value of chirality κ is plotted with respect to the wavelength in Fig. 3(d). It is also found that the value of χ (not shown) is equal to zero.

#95702 - $15.00 USD Received 2 May 2008; revised 29 Jun 2008; accepted 1 Jul 2008; published 23 Jul 2008

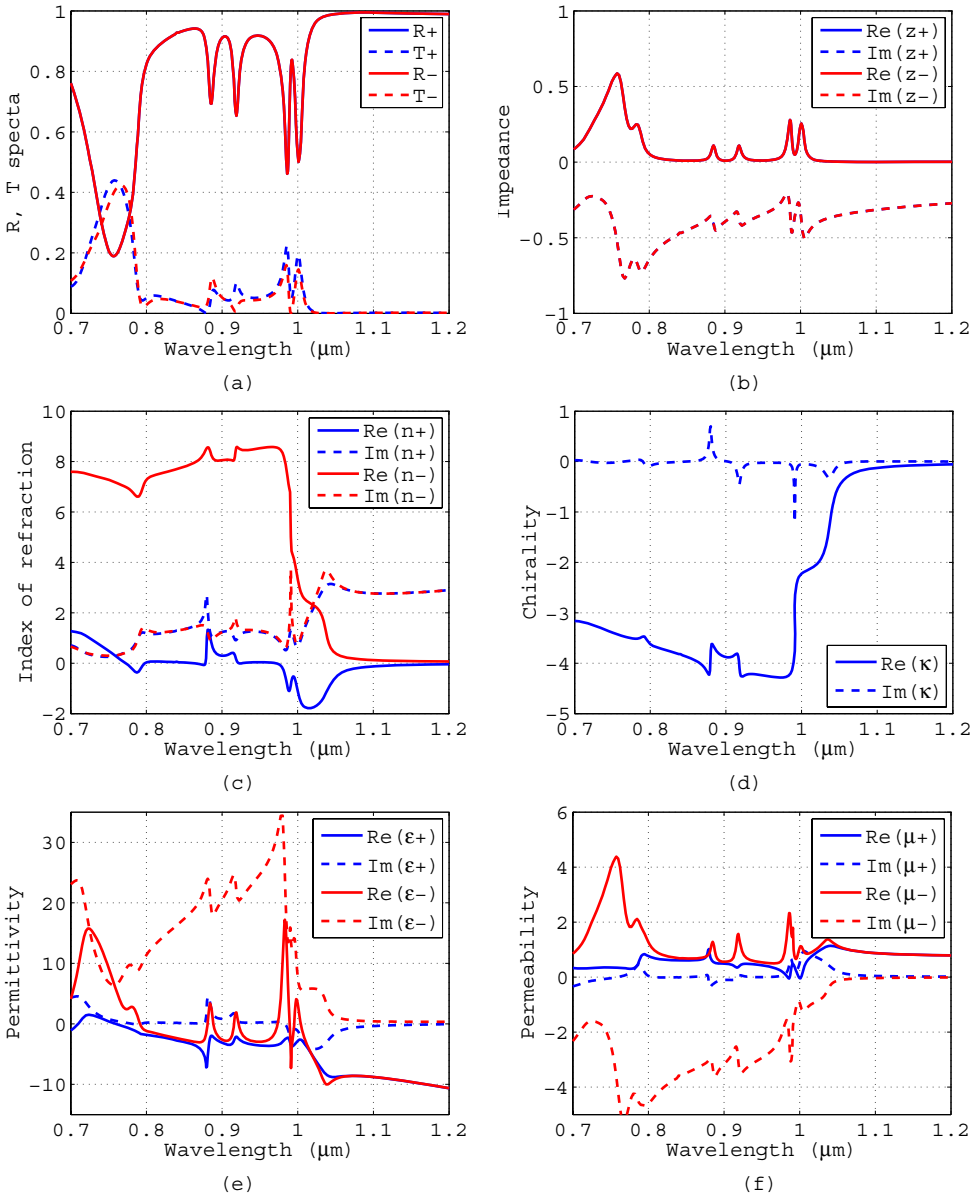

Fig. 3. (Color online) The spectra and material parameters of the chiral optical metamaterial: (a) $R_{\pm}$ and $T_{\pm}$ (reflectance and transmittance), (b) $z_{\pm}$, (c) $n_{\pm}$, (d) κ, (e) $\varepsilon_{\pm}$, and (f) $\mu_{\pm}$.

#95702 - $15.00 USD Received 2 May 2008; revised 29 Jun 2008; accepted 1 Jul 2008; published 23 Jul 2008

The metamaterial behaves as a NIM only for the RCP wavefield over the wavelength range 0.978–1.11 μm. Since the real part of n according to (11) never reaches negative values, it is concluded that the structural chirality built into the metamaterial design plays a critical role in realizing a negative index band for the RCP wavefield.

The effective permittivity $\varepsilon_{\pm}$ and the effective permeability $\mu_{\pm}$ are plotted with respect to wavelength for the two circularly polarized wavefields in Figs. 3(e)–(f). Aside from several resonances observed within the band, one can note that both $\varepsilon_{\pm}$ are negative and overall decreasing functions of wavelength. In the range $\lambda \geq 1.1$ μm (also beyond 1.2 μm), the values of $\varepsilon_{\pm}$ are practically the same and are monotonically decreasing with respect to increasing wavelength. This frequency-scaled Drude-type response is characteristic of continuous metal mesh structures typically found in non-chiral optical NIM designs such as the one reported in [4]. Figure 3(e) indicates that the design relies on a silver mesh that is connected across cell boundaries to produce the desired negative permittivities. To verify the role of the continuous silver mesh in this chiral metamaterial design, a numerical experiment was performed where the metallic mesh was broken and a narrow air gap was inserted between each of the quadrants comprising a unit cell (see the dashed contours shown in Fig. 2(c) indicating where the air gaps were placed). As expected, with the silver layers disconnected, the Drude-type behavior responsible for the negative values of $\varepsilon_{\pm}$ disappeared.

Figure 3(f) clearly shows the polarization-sensitive magnetic resonance of the chiral metamaterial. The most important distinction occurs around $\lambda = 1.0$ μm, where μ_{+} sharply decreases and μ_{-} increases from unity as the wavelength is decreased. These polarization-sensitive resonances combined with the negative permittivities associated with the continuous silver layers are responsible for the negative index for the RCP wavefield and the positive index for the LCP wavefield, leading to the large chirality parameter shown in Fig. 3(d).

5. Conclusion

A material parameter extraction procedure for general BI metamaterials has been presented. The retrieved material parameters correspond to those of the homogeneous BI material slab of the same thickness that produces the same transmission and reflection properties. A doubly-periodic chiral NIM design in the near-IR spectrum has also been presented along with the extracted material parameters. The design is realized by arranging the conventional metal-dielectric-metal resonators in a helical (i.e., stair-step) fashion within a quadrant of the unit cell and enforcing the rotational symmetry on the unit cell geometry. A rigorous full-wave numerical analysis shows that the near-IR chiral metamaterial exhibits a negative index band for the RCP component.

Acknowledgments

This work was supported in part by the Penn State Materials Research Institute and the Penn State MRSEC under NSF Grant No. DMR 0213623, and also in part by ARO-MURI award 50342-PH-MUR.

#95702 - $15.00 USD Received 2 May 2008; revised 29 Jun 2008; accepted 1 Jul 2008; published 23 Jul 2008